Chinese Journal of
POLYMER SCIENCE

RESEARCH ARTICLE

https://doi.org/10.1007/s10118-023-2941-3
Chinese J. Polym. Sci. **2023**, *41*, 956–961

Decreasing the CTE of Thermoplastic Polyimide by Blending with a Thermosetting System

Yu-Cheng Zi[a], Gao-Jie Wu[a], Dong-Xu Pei[a], Shu Guo[b], Sheng-Li Qi[a], Guo-Feng Tian[a*], and De-Zhen Wu[a]

[a] *Key Laboratory of Carbon Fiber and Functional Polymers (Beijing University of Chemical Technology), Ministry of Education, Beijing 100029, China*
[b] *Institute of Analysis and Testing, Beijing Academy of Science and Technology (Beijing Center For Physical & Chemical Analysis), Beijing 100089, China*

Abstract A series of thermoplastic polyimide resins with a low coefficient of thermal expansion (CTE) were prepared by blending a rigid resin system 3,3',4,4'-biphenyltetracarboxylic dianhydride (BPDA)/*p*-phenylenediamine (PDA) with a flexible resin system 4,4'-[isopropylidenebis(*p*-phenyleneoxy)]diphthalic anhydride (BPADA)/PDA. The effects of the blending ratio on the macromolecular coil size, free volume, and CTE of the mixed system were studied. The mixing is carried out in the prepolymer poly(amide acid) (PAA) stage, which makes the two systems more compatible and is conducive to the formation of a semi-interpenetrating network structure between the rigid molecular chains and flexible molecular chains. The flexible structure of the BPADA/PDA system is used to ensure the melt processing performance. The rigid characteristics of the BPDA/PDA system can inhibit the movement of molecular chains and reduce the free volume fraction, thereby reducing the CTE value. When the rigid system content reaches 30%, the CTE can be reduced to 38 ppm/K. This method provides a new approach for studying low CTE thermoplastic polyimide resins.

Keywords Coefficient of thermal expansion (CTE); Thermoplastic polyimide; Melt processing property; Blending

Citation: Zi, Y. C.; Wu, G. J.; Pei, D. X.; Guo, S.; Qi, S. L.; Tian, G. F.; Wu, D. Z. Decreasing the CTE of thermoplastic polyimide by blending with a thermosetting system. *Chinese J. Polym. Sci.* **2023**, *41*, 956–961.

INTRODUCTION

Thermoplastic polyimide (PI) resins play an important role in the mechanical industry, medical treatment, chemical industry, and other fields due to the outstanding comprehensive performance of the PI material and the good melt processing performance of the thermoplastic resin.[1–4] It can not only be used to prepare advanced composite materials[5–7] but also to prepare medical sterilization packaging, gears, bearings, *etc*.[8,9] Thermoplastic PI usually chooses flexible monomers to ensure good melt processing performance, such as 4,4'-oxydiphthalic anhydride (ODPA) and 4,4'-diaminodiphenyl ether (ODA), to improve the movement of the molecular chain.[10–12] However, flexible molecular chains usually lead to a high coefficient of thermal expansion (CTE) due to the movement of the molecular chain and the unordered arrangement.[13–15] For example, the CTE of a typical thermoplastic PI resin ULTEM is about 56 ppm/K. The high CTE limits the application of the thermoplastic PI resin in the precision device field, such as optical lenses and communication components. Also, other components may slip and even fall off with climate change and electrical heating during use.[16,17] Therefore, the development of methods to reduce the CTE of thermoplastic PI resins has become a new research direction.

There have been many studies on low CTE PI materials, such as using rigid monomers to inhibit the movement of molecular chains,[18,19] adjusting the density of the electron cloud of dianhydride and diamine to increase the probability of charge transfer complex (CTC) formation,[20,21] using strong non-bond interactions such as hydrogen bonds to enhance the intermolecular force,[22,23] and filling rigid nanoparticles.[24,25] However, the methods above will lead to the decrease in the molecular chain movement and the increase in the melt viscosity for the resin, so these methods are mostly used in the film materials prepared by solution molding. Similar to the design contradiction between the low CTE and thermoplastic processing characteristics in PI materials research, there is a design contradiction between the low permittivity and low CTE,[26,27] low CTE and high transmission,[28,29] *etc*. Fang and coworkers prepared a block copolyimide to perform characteristics of each unit, improved the equilibrium properties of the random copolymerization, and achieved the high transparency and low CTE at the same time.[30] Starting from this idea, we consider upgrading the rigid and flexible skeleton structure design to the condensed matter level, blending at the molecular chain state, working the respective roles of flexible and rigid systems, and realizing the balance between the thermoplastic processing characteristics and the low CTE value.

Therefore, we chose BPADA/PDA as the flexible main structure and BPDA/PDA as the rigid main structure to blend in the polyamide acid stage. This not only avoids the problem that the uniform distribution of rigid monomers affects the motil-

* Corresponding author, E-mail: tiangf@mail.buct.edu.cn
Received October 18, 2022; Accepted December 26, 2022; Published online March 3, 2023

ity in the process of copolymerization but also promotes the full mutual capacity of the two systems at the molecular chain level, which is conducive to the formation of a network structure with interpenetrating rigid and flexible molecular chains. This mechanism is shown in Fig. 1. The good melt processing performance of the BPADA/PDA flexible system was used to realize the requirements of thermoplastic processing, and the anchoring effect of the rigid BPDA/PDA system was used to reduce the movement of the molecular chain inside the formed product and the free volume fraction inside the system in order to reduce the CTE value of the product.

EXPERIMENTAL

Materials

The monomers BPADA, BPDA and PDA were provided by Beijing Forsman Technology Co., LTD. The solvent *N*,*N*-dimethylacetamide (DMAc) was purchased from Tianjin Damao Chemical Reagent Factory. Both pyridine and acetic anhydride are commercially available analytical pure products and used as received without further purification.

Preparation Process of PI Resins

Taking (BPADA/PDA):(BPDA/PDA)=7:3 (*W*:*W*) as an example. BPADA (5.889 g, 11.3 mmol) was added into a 250 mL three-necked flask, and then 70 mL of DMAc was added and stirred until the dianhydride monomer was completely dissolved. Then, PDA (1.111 g, 10.3 mmol) was added in batches, and the PAA solution (1 g/10mL) was obtained by reaction in an ice bath for 2 h. Meanwhile, in another 100 mL three-necked flask, BPDA (2.249 g, 8 mmol), DMAc (30 mL) and PDA (0.751 g, 7.2 mmol) were added in order, and the PAA solution (1 g/10mL) was obtained by the same procedure. Then, the two PAA solutions were mixed and stirred for 8 h. Pyridine and acetic anhydride were added to carry out chemical imidization, and the reaction continued for 2 h. Finally, the solution was slowly dropped into the stirring ethanol to precipitate a yellowish solid, filtrated and washed with ethanol, and placed in the oven for 2 h at 260 °C to complete the imidization. The PI resins were set as BPADA/PDA, (BPADA/PDA):(BPDA/PDA)=9:1, (BPADA/PDA):(BPDA/PDA)=8:2, and (BPADA/PDA):(BPDA/PDA)=7:3 according to the blending ratio and named as BPADA/PDA, PI-9:1, PI-8:2, and PI-7:3 for short.

Preparation of PI Sheets

The PI sheets were prepared by hot-press according to the heating procedure shown in Fig. 2. The PI resin powder was kept at 260 °C for 20 min and then heated to 320 °C for 20 min. During the hot-pressing process, the pressure was maintained at 2 MPa and the pressure was relieved several times to discharge the air as much as possible.

Measurements

Fourier transform infrared spectroscopy (FTIR) was performed by using the Nexus 670 (Nicolet Company, USA) with the scanning wavenumbers ranging from 4000 cm^{-1} to 400 cm^{-1}.

The differential scanning calorimetry (DSC) test was performed on a Q20 (TA Company, USA). In the nitrogen environment, the resin was heated to 400 °C at the rate of 10 °C/min and then lowered to room temperature after holding for 5 min. Then, the resin was heated to 400 °C at the rate of 10 °C/min again to observe the heat absorption and release of the resin and to record the data at the same time.

The viscous flow characterization for the PI resins was conducted on the hybrid rheometer DHR-1 (TA Company, USA) equipped with a 25 mm diameter parallel plate fixture. The PI

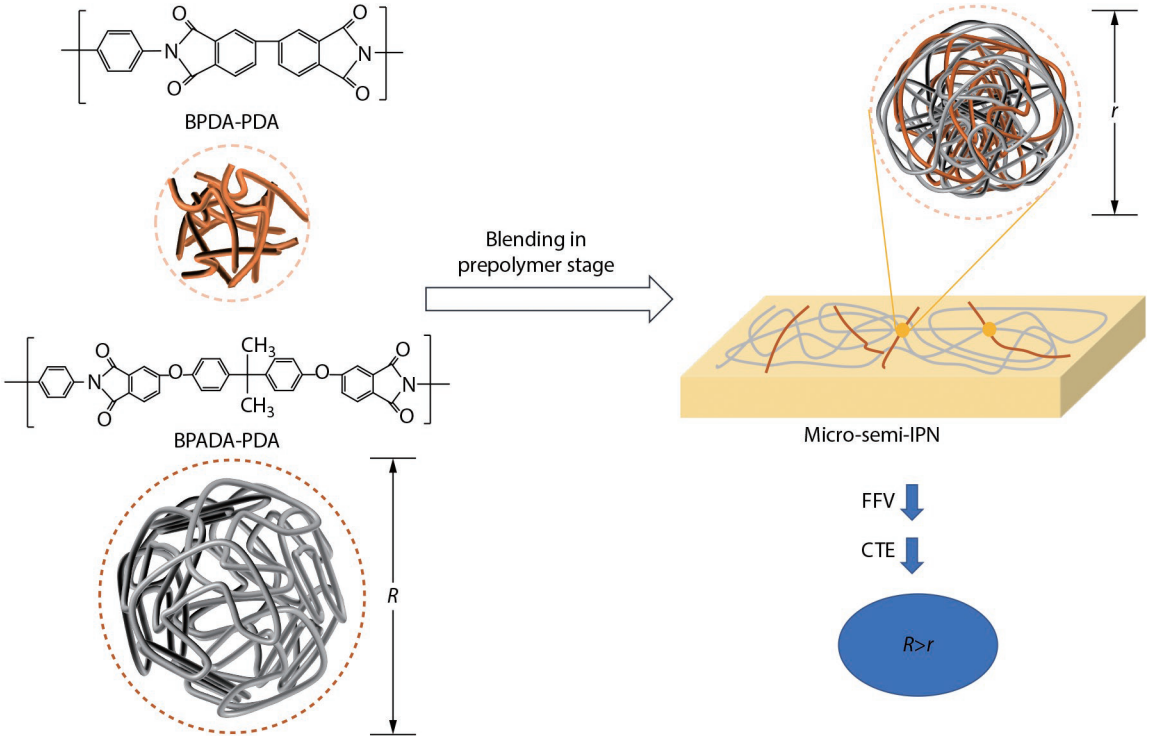

Fig. 1 Interpenetration mechanism of rigid and flexible molecular chains.

https://doi.org/10.1007/s10118-023-2941-3

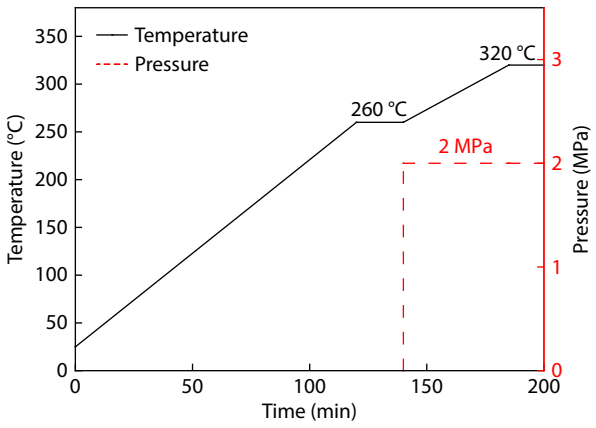

Fig. 2 Hot molding process for the PI resin.

resin was pressed into φ=25 mm, h=1 mm discs for the test and heated to 400 °C at a rate of 5 °C/min. The test conditions were oscillation mode, a frequency of 10 Hz, a strain of 0.1%, and an oscillation frequency of 10 rad/s.

The particle size and distribution of the PAA solution were determined by using the Zetasizer Nano (Malvern Company, UK). The concentration of the PAA solution was 2 mg/mL, the test temperature was 20 °C, and the solution was stable for 120 s before the test.

The CTE of the PI resin was determined by using the Q400 (TA Company, USA). The thermal history was eliminated by heating from room temperature to 100 °C at a rate of 5 °C/min in a N_2 atmosphere. After cooling completely, the temperature was increased a second time to 100 °C at a rate of 5 °C/min to calculate the CTE value of the PI resin.

The molecular simulation technique was used to analyze the occupied volume and free volume distributions and to calculate the free volume fraction (FFV) and CTE. This calculation process was performed by Materials Studio 8.0, and the detailed method was based on our previous work.[26,31,32]

RESULTS AND DISCUSSION

Fourier Transform Infrared Spectrometry (FTIR)

The FTIR spectra of PI resins with different blending ratios are presented in Fig. 3. The characteristic absorption bands at 1780 and 1720 cm^{-1} ascribed to asymmetric and symmetric stretching vibration bands of carbonyl C=O on the imide ring can be seen. The characteristic absorption bands around 1370 cm^{-1} correspond to the C—N bond, and the characteristic absorption bands at 720–740 cm^{-1} are ascribed to the C=O bending vibration. These results indicate that polyimide has been prepared successfully.

Viscous Flow Characterization

The viscosity-temperature curves of BPADA/PDA resins with theoretical molecular weights of 60000, 30000, and 6000 are shown in Fig. 4(a). The melt viscosity decreased with the reduction in the molecular weight, and the minimum viscosity decreased from 9689 Pa·s with a theoretical molecular weight of 60000 to 144 Pa·s with the theoretical molecular weight of 6000. This is mainly due to the decrease in the molecular weight, which makes the molecular chain shorter, and the number of chain ends increases while the entanglement effect is weakened. Compared with the structural units, the chain ends have a larger free volume and stronger mobility, so the melt viscosity decreases.

The BPADA/PDA system with the lowest melt viscosity and theoretical molecular weight of 6000 was selected as the matrix to blend with different amounts of BPDA/PDA. The visco-

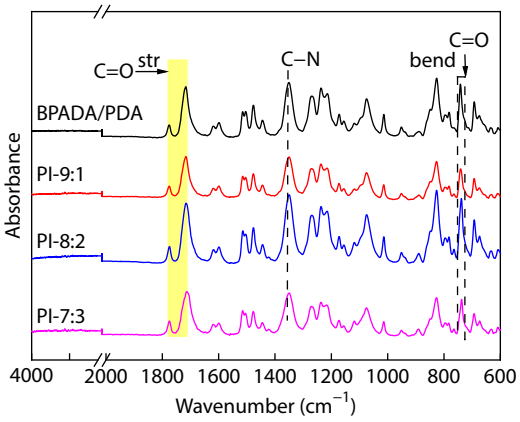

Fig. 3 FTIR spectra of PI resins of different blending ratios.

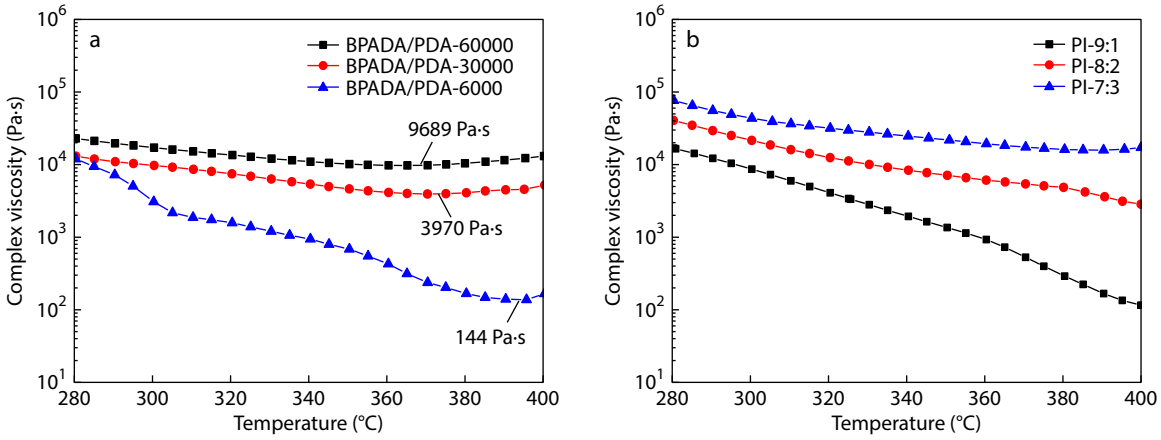

Fig. 4 (a) Viscosity-temperature curves of BPADA/PDA with different molecular weights; (b) The viscosity-temperature curves of BPADA/PDA and BPDA/PDA resins with different blending ratios.

https://doi.org/10.1007/s10118-023-2941-3

sity-temperature curves of the blending PI resins are shown in Fig. 4(b). The melt viscosity increased with the increase in the amount of rigid component BPDA/PDA. This is mainly because of the high rigidity of the BPDA/PDA system and the poor motility of the molecular chains.

Differential Scanning Calorimetry (DSC)

The DSC test results of the PI resins are shown in Fig. 5. The glass transition temperature of BPADA/PDA is 233 °C. Due to the rigid skeleton structure of the BPDA/PDA chain and the limited movement of the chain segments, the glass transition of BPDA/PDA could not be observed in the DSC test. This is the reason why only one glass transition temperature appears in the blending systems. With the increase in the rigid component BPDA/PDA content, the glass transition temperature of the blended PI system increased gradually from 233 °C in the BPADA/PDA system to 243 °C in the PI-7:3 system. This phenomenon indicates that BPDA/PDA does play a positive role in restricting the movement of BPADA/PDA chain segments and increasing the glass transition temperature of the blend system. It can also be inferred that the interaction scale of the two PI systems may be at the chain segment level.

Size of Coil

A laser particle size analyzer was used to test the particle size of each system in the PAA solution stage. In order to avoid entanglement and overlap of molecular chains caused by an excessive concentration, the solution was diluted to 2 mg/mL to obtain a relatively independent size of the coil as much as possible. The test results are shown in Fig. 6 and Table 1. As can be seen from Figs. 6(a) and 6(b), the size of the polymer coil of PAA in the two systems increased with the increasing molecular weight. In addition, the conformational rotation of the BPADA/PDA chain was stronger than that of the BPDA/PDA system, which is attributed to the presence of ether bonds. Therefore, the coil size of the BPADA/PDA system is smaller than that of the BPDA/PDA system with a similar molecular weight.

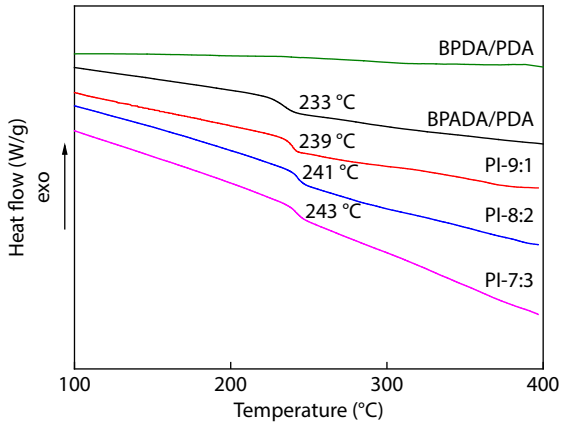

Fig. 5 DSC curves of PI resins with different blending ratios.

BPADA/PDA with a molecular weight of 6000 was used as the matrix and blended with BPDA/PDA. From Fig. 6(c), it can be observed that the two blending systems do not show two

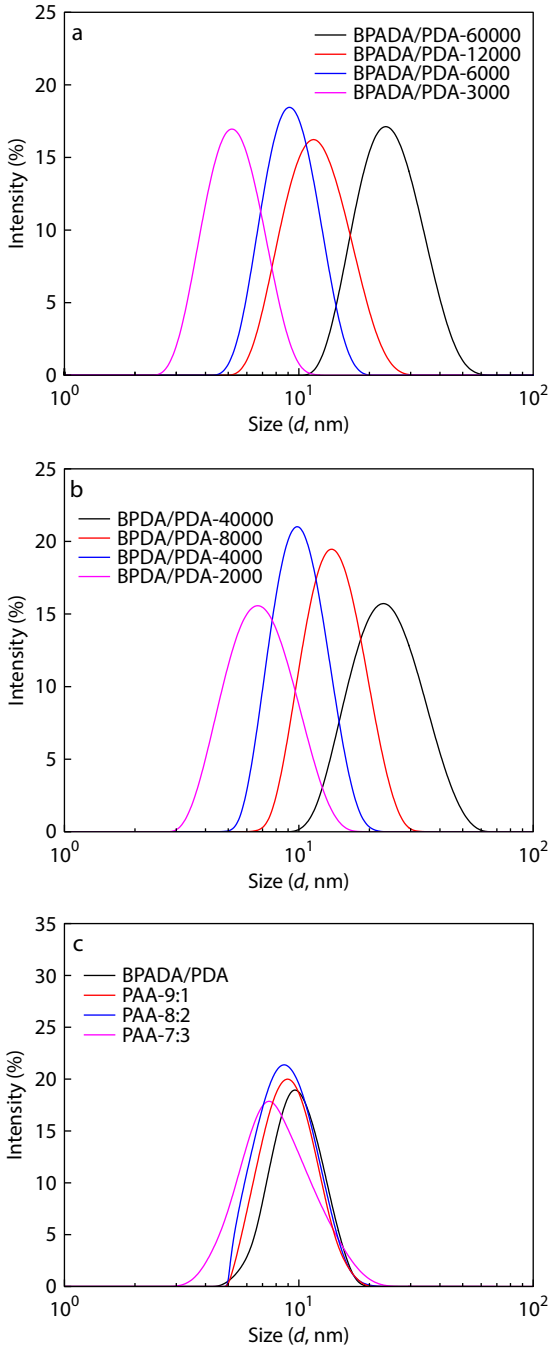

Fig. 6 Particle size distribution of different PAA dilute solutions: (a) BPADA/PDA, (b) BPDA/PDA, (c) BPADA/PDA&BPDA/PDA.

Table 1 The coil size of each PI system.

Sample	Size (nm)	Sample	Size (nm)	Sample	Size (nm)
BPADA/PDA-60000	24.4	BPDA/PDA-40000	21.0	PAA-9:1	9.1
BPADA/PDA-12000	11.7	BPDA/PDA-8000	11.7	PAA-8:2	8.7
BPADA/PDA-6000	9.3	BPDA/PDA-4000	8.7	PAA-7:3	7.5
BPADA/PDA-3000	4.9	BPDA/PDA-2000	5.6	/	/

https://doi.org/10.1007/s10118-023-2941-3

particle sizes but rather one coil size. With the increase in the BPDA/PDA content, the coil size of the blending system decreased gradually from 9.3 nm of BPADA/PDA-6000 to 7.5 nm when the blending ratio was 7:3. These results further indicate that the molecular chains of the two systems achieve a molecular level mutual solution, which may form a network structure of rigid and flexible molecular chains interspersed with each other.

CTE

The curve of the PI resin sheet deformation changing with temperature is shown in Fig. 7 and Table 2. As can be seen from the data, the CTE of BPADA/PDA is 56 ppm/K, which is similar to that of the ULTEM resin. The CTE of the blended PI decreased with the increase in the BPDA/PDA content. The CTE decreased from 56 ppm/K of BPADA/PDA to 38 ppm/K of PI-7:3, which is a drop of more than 30%. Material Studio 8.0 was used to calculate the CTE of the blending PI system. The calculated result is shown in Table 2. Although the calculated results are higher than the experimental results, the overall reduction trend is basically the same, which further validates the design idea of blending a rigid and flexible system to reduce the CTE of the PI resin.

FFV

Materials Studio was used to calculate the FFV of each blend system when BPADA/PDA blends with BPDA/PDA. The results are shown in Fig. 8 and Table 3. It can be seen from the data that the FFV of BPADA/PDA is 37.5%. The FFV of the blending system decreased gradually with the addition of the rigid component BPDA/PDA. This could be because the BPADA/PDA and BPDA/PDA systems form a similar semi-interpenetrating network structure. BPDA/PDA was inserted into the BPADA/PDA system like a rigid rod, which reduced the free volume fraction of the mixing system. The mechanism is shown in Fig. 1, which is basically consistent with the rule of the size change of the coil.

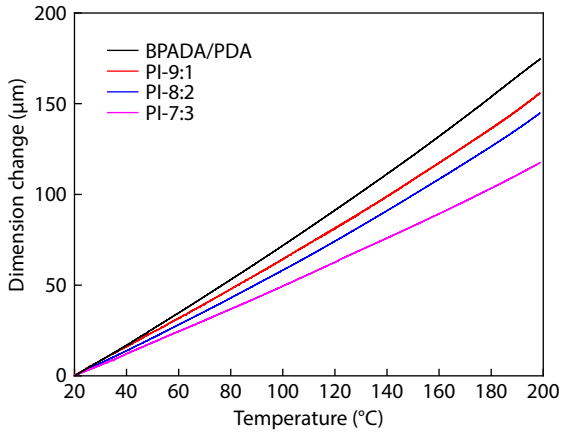

Fig. 7 The CTE curves of PI resins with different blending ratios.

Table 2 The CTE result of PI resins with different blending ratios.

Sample	CTE (20–100 °C) (ppm/K)	
	Experimental data	Simulated result
BPADA/PDA	56	76
PI-9:1	49	58
PI-8:2	45	53
PI-7:3	38	48

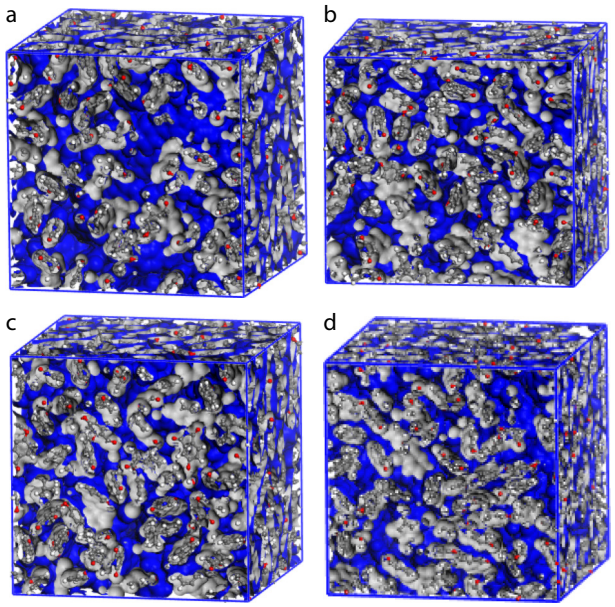

Fig. 8 Free volume distribution diagram: (a) BPADA/PDA, (b) PI-9:1, (c) PI-8:2, (d) PI-7:3. Blue part is free volume, gray part is occupied volume.

Table 3 Free volume of the blending system.

Sample	Occupied volume (Å^3)	Free volume (Å^3)	FFV (%)
BPADA/PDA	50314.5	30188.7	37.5
PI-9:1	46955.7	27814.5	37.2
PI-8:2	44133.9	25808.9	36.9
PI-7:3	43052.7	24853.8	36.6

CONCLUSIONS

A series of thermoplastic PI resins with melt processing properties and low CTE were prepared by blending the flexible system BPADA/PDA and the rigid system BPDA/PDA at the prepolymer stage. The flexible system BPADA/PDA was selected to ensure the melt processing performance of the resin. The rigid system BPDA/PDA intermixed with the flexible system can reduce the FFV of the blended system on the one hand and inhibit the movement ability of the flexible system chain segment on the other hand, so that the glass transition temperature is increased and the CTE is reduced. When the addition of BPDA/PDA reached 30%, the CTE of the blending resin decreased from 56 ppm/K to 38 ppm/K, a drop of more than 30%. This work provides a new idea for reducing the CTE of thermoplastic resins.

NOTES

The authors declare no competing financial interest.

ACKNOWLEDGMENTS

This work was financially supported by the National Natural Science Foundation of China (No. 51773007) and the

Fundamental Research Funds for the Central Universities (No. XK1802-2).

REFERENCES

1 Imaizumi, S.; Ohtsuki, Y.; Yasuda, T. Printable polymer actuators from ionic liquid, soluble polyimide, and ubiquitous carbon materials. *ACS Appl. Mater. Interfaces* **2013**, *5*, 6307–6315.
2 Kim, I. C.; Park, K. W.; Tak T. M. Synthesis and characterization of soluble polyimides and its ultrafiltration membrane performances. *J. Appl. Polym. Sci.* **1999**, *73*, 907–918.
3 Mittal, K. L. Polyimides: synthesis, characterization, and applications. *Polym. Compos.* **1982**, *3*, 245.
4 Makino, D. Application of polyimide resin to semiconductor devices in Japan. *IEEE. Electr. Ins. Mag.* **1988**, *4*, 15–23.
5 Shukla, P.; Saxena, P. Polymer nanocomposites in sensor applications: a review on present trends and future scope. *Chinese J. Polym. Sci.* **2021**, *39*, 665–691.
6 Mustafa, C.; Emre, A. Characterization of carbon fiber-reinforced thermoplastic and thermosetting polyimide matrix composites manufactured by using various synthesized PI precursor resins. *Compos. Part B-Eng.* **2022**, *231*, 109559.
7 Xu, J.; Huang, X.; Davim, J. P.; Ji, M.; Chen, M. On the machining behavior of carbon fiber reinforced polyimide and PEEK thermoplastic composites. *Polym. Compos.* **2020**, *41*, 3649–3663.
8 Ye, W. L.; Wu, W. Z.; Hu, X.; Lin, G. G. 3D printing of carbon nanotubes reinforced thermoplastic polyimide composites with controllable mechanical and electrical performance. *Compos. Sci. Technol.* **2019**, 182, 107671.
9 Byberg, K. I.; Gebisa, A. W.; Lemu, H. G. Mechanical properties of ULTEM 9085 material processed by fused deposition modeling. *Polym. Test.* **2018**, *72*, 335–347.
10 Hu, J.; Wang, J.; Qi, S. Thermoplastic and soluble co-polyimide resins fabricated *via* the incorporation of 2,3,3′,4′-biphenyltetracarboxylic dianhydride. *High. Perform. Polym.* **2019**, *31*, 1272–1279.
11 Yi, L.; Li, C.; Huang, W. Soluble polyimides from 4,4′-diaminodiphenyl ether with one or two *tert*-butyl pedant groups. *Polymer* **2015**, *80*, 67–75.
12 Kim, S. D.; Lee, S.; Heo, J. Soluble polyimides with trifluoromethyl pendent groups. *Polymer* **2013**, *54*, 5648–5654.
13 Sensui, N.; Ishii, J.; Takata, A. Ultra-low CTE and improved toughness of PMDA/PDA polyimide-based molecular composites containing asymmetric BPDA-type polyimides. *High. Perform. Polym.* **2009**, *21*, 709–728.
14 Hasegawa, M.; Watanabe, Y.; Tsukuda, S. Solution-processable colorless polyimides with ultralow coefficients of thermal expansion for optoelectronic applications. *Polym. Int.* **2016**, *65*, 1063–1073.
15 Yi, J.; Liu, C.; Tian, Y.; Wang, K.; Liu, X.; Luo, L. Improving dimensional stability at high temperature and toughness of polyimide films *via* adjustable entanglement density. *Polymer* **2021**, *218*, 123488.
16 Gao, G.; Mao, D.; Fan, B.; Guan, C. Effect of wet expansion behavior on polyimide membrane diffractive lens. *Coatings* **2019**, *9*, 559.
17 Yin, J.; Mao, D.; Fan, B. Copolyamide-imide membrane with low CTE and CME for potential space optical applications. *Polymers* **2021**, *13*, 1001.
18 Jung, Y.; Yang, Y.; Kim, S. Structural and compositional effects on thermal expansion behavior in polyimide substrates of varying thicknesses. *Eur. Polym. J.* **2013**, *49*, 3642–3650.
19 Tan, Y.; Zhang, Y.; Jiang, G. Preparation and properties of inherently black polyimide films with extremely low coefficients of thermal expansion and potential applications for black flexible copper clad laminates. *Polymers* **2020**, *12*, 576.
20 Yu, X. H.; Liu, J. N.; Wu, D. Y. Colorless PI structure design and evaluation for achieving low CTE target. *Mater. Today Commun.* **2019**, *21*, 100562.
21 Yang, Z.; Guo, H.; Kang, C. Synthesis and characterization of amide-bridged colorless polyimide films with low CTE and high optical performance for flexible OLED displays. *Polym. Chem.* **2021**, *12*, 5364–5376.
22 Mushtaq, N.; Wang, Q.; Chen, G. Synthesis of polyamide-imides with different monomer sequence and effect on transparency and thermal properties. *Polymer* **2020**, *190*, 122218.
23 Bai, L.; Zhai, L.; He, M. H. Thermal expansion behavior of poly(amide-imide) films with ultrahigh tensile strength and ultralow CTE. *Chinese J. Polym. Sci.* **2020**, *38*, 748–758.
24 Tsai, M. H.; Huang, Y. C.; Tseng, I. H. Thermal and mechanical properties of polyimide/nano-silica hybrid films. *Thin Solid. Films.* **2011**, *519*, 5238–5242.
25 Luo, J.; Wu, Y.; Sun, Y.; Wang, G.; Liu, Y.; Zhao, X.; Ding, G. Preparation and characterization of high thermal conductivity and low CTE polyimide composite reinforced with diamond nanoparticles/SiC whiskers for 3D IC interposer RDL dielectric. *Appl. Sci.* **2019**, *9*, 1962.
26 Zhou, H.; Lei, H.; Wang, J. Breaking the mutual restraint between low permittivity and low thermal expansion in polyimide films *via* a branched crosslink structure. *Polymer* **2019**, *162*, 116–120.
27 Han, S.; Li, Y.; Hao, F. Ultra-low dielectric constant polyimides: Combined efforts of fluorination and micro-branched crosslink structure. *Eur. Polym. J.* **2021**, *143*, 110206.
28 Zhi, X.; Jiang, G.; Zhang, Y. Preparation and properties of colorless and transparent semi-alicyclic polyimide films with enhanced high-temperature dimensional stability *via* incorporation of alkyl-substituted benzanilide units. *J. Appl. Polym. Sci.* **2022**, *139*, 51544.
29 Peng, W. F.; Lei, H. Y.; Zhang, X. X. Fluorine substitution effect on the material properties in transparent aromatic polyimides. *Chinese J. Polym. Sci.* **2022**, *40*, 781–788.
30 Lao, H.; Mushtaq, N.; Chen, G. Synthesis and properties of transparent random and multi-block polyamide-imide films with high modulus and low CTE. *Eur. Polym. J.* **2021**, *153*, 110512.
31 Li, X.; Lei, H.; Guo, J.; Wang, J. Composition design and properties investigation of BPDA/PDA/TFDB co-polyimide films with low dielectric permittivity. *J. Appl. Polym. Sci.* **2019**, *136*, 47989.
32 Hao, F. Y.; Wang, J. H.; Qi, S. L. Structures and properties of polyimide with different pre-imidization degrees. *Chinese J. Polym. Sci.* **2020**, *38*, 840–846.

https://doi.org/10.1007/s10118-023-2941-3